PERGAMON

European Journal of Cancer 37 (2001) 1173–1180

European Journal of Cancer

www.ejconline.com

Different effects of methotrexate on DNA mismatch repair proficient and deficient cells

I. Frouin [a], E. Prosperi [b], M. Denegri [a], C. Negri [a], M. Donzelli [a], L. Rossi [a], F. Riva [b], M. Stefanini [a], A.I. Scovassi [a,*]

[a] *Istituto di Genetica Biochimica ed Evoluzionistica del C.N.R., Via Abbiategrasso 207, I-27100 Pavia, Italy*
[b] *Centro di Studio per l'Istochimica del C.N.R., Piazza Botta 10, I-27100 Pavia, Italy*

Received 19 December 2000; received in revised form 6 February 2001; accepted 28 February 2001

Abstract

Antifolates exert their antiproliferative activity through the inhibition of dihydrofolate reductase and, as a consequence, of thymidylate synthesis, thereby inducing nucleotide misincorporation and impairment of DNA synthesis. We investigated the processes involved in the repair of antifolate-induced damage and their relationship with cell death. Since misincorporated bases may be removed by DNA mismatch repair (MMR), the study was carried out on the MMR-proficient human cell lines HeLa and HCT116 + chr3, and, in parallel, on the MMR-deficient cell lines HeLa cell-clone12, defective in the protein hPMS2, and HCT116, with an inactive hMLH1. After treatment with methotrexate (MTX), we observed that DNA repair synthesis occurs independently of the cellular MMR function. Clear signs of apoptosis such as nuclear shrinkage, chromatin condensation and degradation, DNA laddering, and poly (ADP-ribose) polymerase (PARP) proteolysis, were visible in both MMR^+ and MMR^- cells. Remarkably, cell viability was lower and the apoptotic process was triggered more efficiently in the MMR-competent cells.

Keywords: Methotrexate; DNA mismatch repair; Base excision repair; Apoptosis; PCNA

1. Introduction

Antifolates such as methotrexate (MTX) are widely used as chemotherapeutic drugs because of their ability to affect cell replication (reviewed in Ref. [1]). Their main target is the enzyme dihydrofolate reductase, whose inhibition leads to the impairment of new DNA synthesis by restriction of the supply of deoxythymidine triphosphate (dTTP) and of purine nucleotides and by the consequent misincorporation of uracil into DNA [2]. As an effect of MTX administration, a cycling process of deoxyuracil monophosphate (dUMP) removal, reincorporation and removal may result in the progressive accumulation of DNA strand breaks [2–4].

The main repair system for removal of misincorporated uracil is the base excision repair [5–8], which requires, for the long-patch subpathway, the proliferating cell nuclear antigen (PCNA) [6,8,10], a protein that plays a crucial role in both DNA replication and repair pathways (reviewed in Refs. [9,10]). In addition, DNA mismatch repair (MMR) is involved in the correction of DNA replication errors [11]. In human cells, this process is strand-specific and it is regulated by the cooperation between the proteins hMSH2, hMSH3, hMSH6, hMLH1, hPMS1 and hPMS2 (reviewed in Refs. [12,13].

The cytotoxic effect of MTX in tumour cells has been extensively investigated, and the activation of the apoptotic pathway in response to this drug has been demonstrated by the presence of typical hallmarks like chromatin condensation, nuclear fragmentation, internucleosomal DNA cleavage and cell cycle perturbations [14,15].

The aim of this study was to gain new insights on the processes involved in the removal of DNA damage induced by MTX, to investigate the relevance of MMR

* Corresponding author. Tel.: +39-0382-546-334/8; fax: +39-0382-422-286.
E-mail address: scovassi@igbe.pv.cnr.it (A.I. Scovassi).

0959-8049/01/$ - see front matter
PII: S0959-8049(01)00095-8

and to clarify the relationships between MMR efficiency, cell viability and apoptosis.

2. Materials and methods

2.1. Cell culture

We used two human MMR-deficient cells: the colon carcinoma cell line HCT116 [17] and the HeLa cell-clone12 [18], as well as two human MMR-proficient cells: HeLa [16], and HCT116 + chr3 where hMLH1 expression was restored by chromosome 3 transfer [17]. Cells were grown as monolayer in Dulbecco's modified Eagle's medium (DMEM, GIBCO-BRL, Paisley, UK) supplemented with 10% fetal calf serum (FCS; HyClone, Logan, UT), 4 mM L-glutamine, 2 mM sodium pyruvate, 100 U/ml penicillin, and 0.1 mg/ml streptomycin (all from GIBCO-BRL). HCT116 + chr3 strain was cultured in the presence of G418 (500 μg/ml, Boehringer). Cells were grown at 37°C in a humidified atmosphere containing 5% CO_2, trypsinised when confluent and split 1:10 in fresh medium.

2.2. Treatments

Stock solution of methotrexate (MTX, amethopterin; Sigma, St Louis, MO, USA) was prepared in 0.1 N NaOH at the concentration of 5 mg/ml. Cells were seeded at 2×10^5 cells/ml, grown in complete medium for up to 48 h and then incubated for 24 h with 50, 150, 250 and 350 μg/ml MTX. After drug removal, cells were washed twice with DMEM, harvested immediately or further cultured in drug-free medium for up to 72 h. Three independent experiments were performed.

2.3. Cell viability

Drug cytotoxicity was evaluated by Trypan blue exclusion assay [20] at the end of each treatment. Cells excluding Trypan blue were considered as viable and counted with a haemocytometer. Viability of different cell lines was compared by the Student's *t*-test using the Statistical Package for the Social Sciences (SPSS) for Windows release 6.0 (SPSS Inc., Chicago, IL).

2.4. Cell cycle analysis

To evaluate the DNA content and the distribution of detergent-insoluble PCNA [21], cells were lysed in hypotonic solution (10 mM Tris–HCl pH 7.5; 2.5 mM $MgCl_2$; 1 mM phenylmethyl sulphonyl fluoride (PMSF); 0.5% Nonidet (N)P40), resuspended in 1 ml of cold 0.9% NaCl and then fixed by adding 2 ml of cold absolute ethanol. Samples were incubated for 1 h with the MAb PC10 (Dako, Denmark) diluted to 5 μg/ml in PBT (phosphate-buffer solution (PBS) containing 1% bovine serum albumin (BSA) and 0.2% Tween 20), washed three times in PBT, and further incubated for 30 min with fluorescein isothiocyanate (FITC)-conjugated anti-mouse IgG (Sigma) diluted 1:100 in PBT. For DNA staining, cells were incubated for 30 min in PBS containing 5 μg/ml propidium iodide and 1 mg/ml RNase A (Sigma). Cells were measured with a Coulter Epics XL flow cytometer (Coulter Co, USA), and statistical analysis of fluorescence intensity signals was performed with the XL2 software. Three independent experiments were carried out.

2.5. Determination of DNA synthesis by BrdU incorporation

According to Stivala and colleagues [22], cells were pulse-labelled with 30 μM bromodeoxyuridine (BrdU) for 1 h at 37°C, resuspended in 1 ml of cold 0.9% NaCl, fixed by adding 2 ml of cold absolute ethanol, incubated for 30 min at room temperature in 2 N HCl, centrifuged and neutralised with 0.1 N sodium tetraborate (pH 8.2) for 15 min. Samples were incubated for 1 h with a MAb anti-BrdU (Progen, Germany) diluted 1:20 in PBT and for 30 min with FITC-conjugated antimouse IgG diluted 1:100 in PBT. Finally, cells were stained with 5 μg/ml propidium iodide in PBS containing 200 μg/ml RNase A. Cell immunofluorescence was measured by flow cytometry, as described above.

2.6. Evaluation of apoptotic features

2.6.1. Cell morphology

At the end of each treatment, 1×10^6 cells were resuspended in 1 ml of cold PBS containing 10% FCS and cytocentrifuged on microscope slides at 500 rotations per minute (rpm) for 3 min at room temperature. After fixation in cold methanol/acetic acid (3:1) for 15 min, cells were washed several times with ice-cold PBS. DNA was stained with 0.1 μg/ml Hoechst 33258 (Sigma) for 10 min at room temperature in the dark. Microscopic observation was carried out using a Leitz Orthoplan microscope equipped with a 50× objective. For each sample, 1000 cells were counted. Cells were photographed using a HP5 film (400 ASA). Four independent experiments were considered to calculate the apoptotic index (A.I.), i.e. the percentage of cells with apoptotic features over the total cell number.

2.6.2. DNA fragmentation

To visualise internucleosomal DNA fragmentation, genomic DNA was rapidly extracted from 2×10^6 cells and analysed by agarose gel electrophoresis as previously reported in Ref. [23].

2.6.3. Poly(ADP-ribose) polymerase proteolysis

Control and treated cells were pelleted, washed twice with ice-cold PBS and resuspended at the concentration of 10×10^6 cells/ml in denaturing buffer containing 62.5 mM Tris–HCl (pH 6.8), 4 M urea, 10% glycerol, 2% sodium dodecyl sulphate (SDS), 5% β-mercaptoethanol and 0.003% bromophenol blue. Western blotting was carried out by using the MAb C-2-10 against poly (ADP-ribose) polymerase (PARP) according to a standard procedure [23].

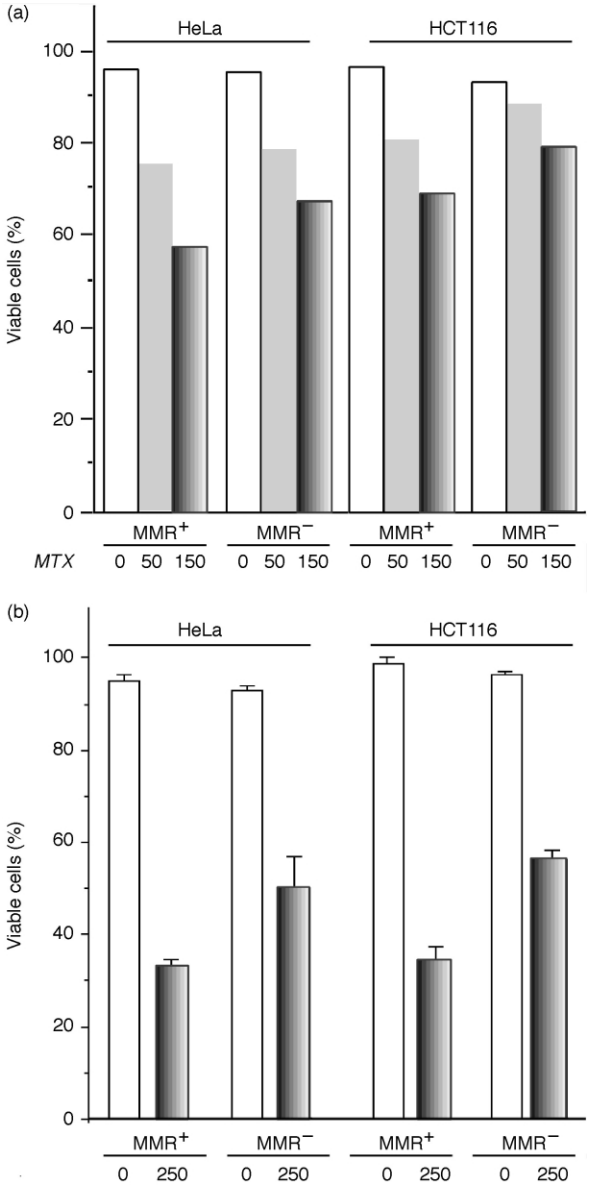

Fig. 1. Effect of methotrexate on the viability of MMR$^+$(HeLa and HCT116+chr3) and MMR$^-$ (HeLa cell-clone12 and HCT116) cell lines. Viable cells in the treated samples were expressed as the percentage of the cell number in the corresponding untreated samples: (a) cells were incubated for 24 h with 50 and 150 μg/ml methotrexate (MTX) and grown in drug-free medium for a further 48 h; (b) treatments were performed with 250 μg/ml (HeLa) or 350 μg/ml MTX. Each value represents the mean of three independent experiments± standard deviation (S.D.).

3. Results

3.1. MTX causes irreversible cytotoxicity

In a first set of experiments, we treated for 24 h both the MMR$^+$ and MMR$^-$ cell lines with increasing doses of MTX (50–350 μg/ml). Under these conditions, cell

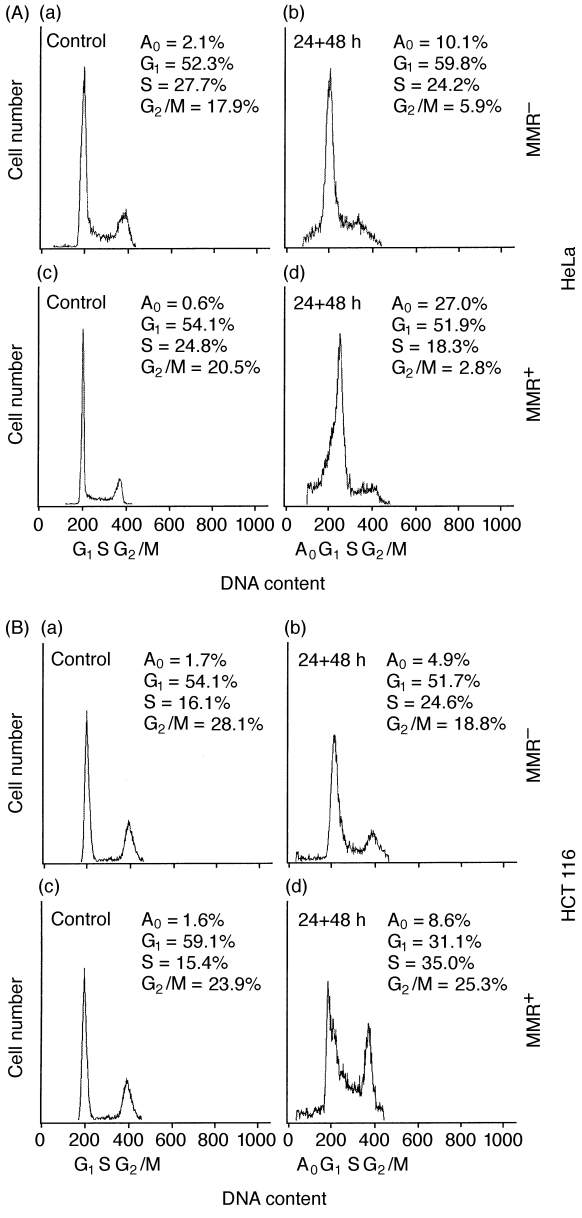

Fig. 2. DNA content of HeLa MMR$^-$ and MMR$^+$ cell lines (A) and HCT116 MMR$^-$ and MMR$^+$ cell lines (B) was measured by flow cytometry. Experiments were performed on untreated samples and in samples cultured for 48 h in normal medium following a 24-h treatment with MTX. Results shown are from one of three independent experiments.

viability (evaluated by Trypan blue exclusion assay) was not significantly affected by the drug (data not shown). To verify whether MTX requires a postincubation time period to display its cytotoxic effect, we have repeated the experiments by incubating the samples for 24 h in drug-free medium after the treatment. These conditions allowed the decrease of viable cells, leading to an ID50 (dose causing 50% inhibition) drug concentration as high as 250 μg/ml for HeLa cells, and 350 μg/ml for HCT116 + chr3 cells (data not shown).

To further understand whether this effect was reversible, we prolonged the recovery time for up to 48 h, and

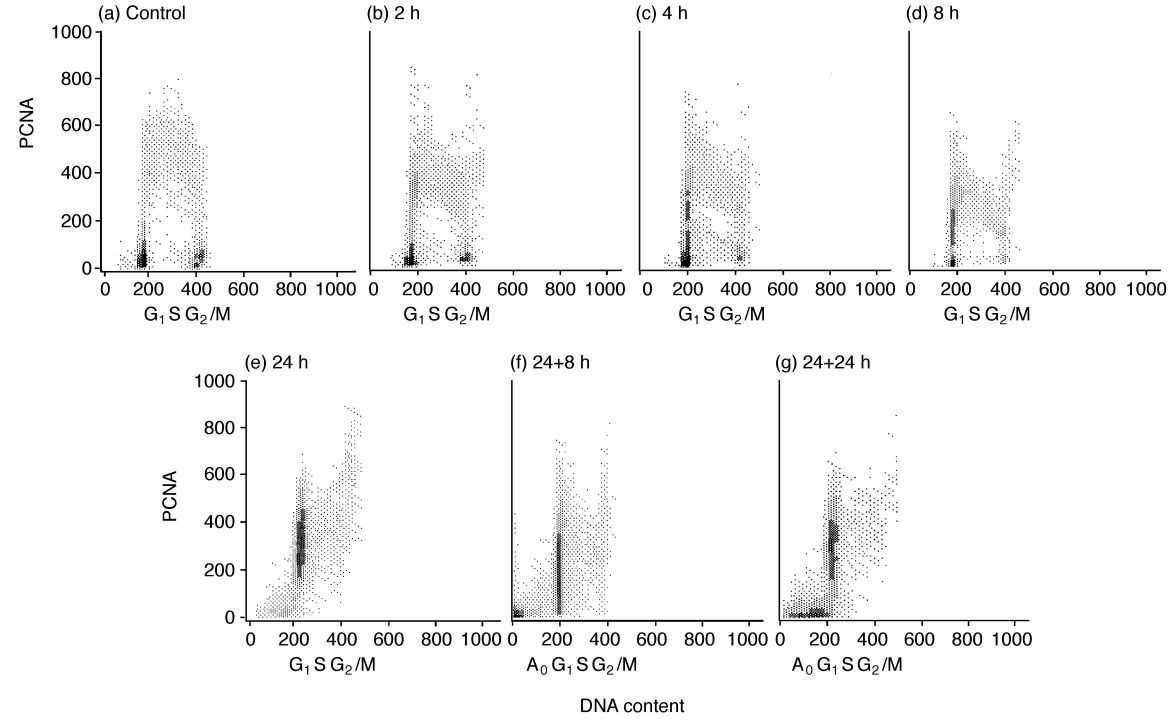

(A) PCNA Immunofluorescence (a.u.)

	Control	2 h	4 h	8 h	24 h	24+8 h	24+24 h
G_1	1.0	2.0	1.8	2.8	7.7	4.9	6.0
S	10.14	10.4	8.0	7.6	9.1	5.9	7.4
G_2/M	1.1	1.5	2.5	5.6	14.8	7.3	10.8

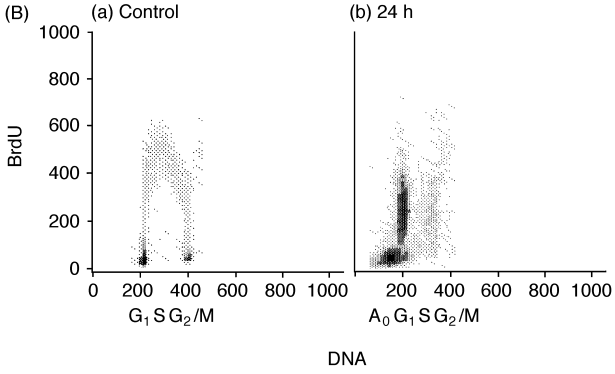

Fig. 3. Cell cycle distribution of nuclear-bound forms of proliferating cell nuclear antigen (PCNA) after MTX-treatment. (A) biparametric dot-plots of PCNA immunofluorescence versus DNA content. HeLa cells were treated with 250 μg/ml MTX for 2 (b), 4 (c), 8 (d) and 24 h (e), and were further incubated in drug-free medium for 8 (f) or 24 h (g). At each experimental point, cells were fixed and analysed by flow cytometry. Quantitation of PCNA immunofluorescence/cell (arbitrary units, a.u.) is reported. (B) Analysis of bromodeoxyuridine (BrdU) incorporation. Biparametric dot-plots of BrdU immunofluorescence versus DNA content were measured in untreated control HeLa cells (a), and in cells treated with 250 μg/ml MTX for 24 h (b). Three independent experiments were performed; the data shown in the figure refer to a typical result.

we found a dose–response effect on cell viability (Fig. 1). The comparison between MMR^+ and MMR^- cell lines treated with 50 and 150 μg/ml MTX, suggested that MMR-deficient cells are less sensitive to the drug (Fig. 1a). Indeed, with a higher MTX concentration (250 μg/ml for the HeLa strains and 350 μg/ml for the HCT116 strains), we found that the MMR-defective HeLa cell-clone12, mutated in hPMS2, was more resistant to MTX than the MMR^+ HeLa parental cell line (Fig. 1b). As determined by Student's *t*-test, the difference was statistically significant (50.00% ± 7.08 versus 33.02% ± 1.70; $P < < 0.001$). Analogously, HCT116 cells, which have mutated hMLH1, showed a cell viability higher than their MMR-proficient derivative HCT116 + chr3 ($P = 0.003$).

3.2. MTX induces cell cycle perturbations

DNA content and cell cycle distribution were analysed in samples incubated for 24 h with 250 μg/ml (HeLa, Fig. 2A) or 350 μg/ml MTX (HCT116, Fig. 2B) and grown in drug-free medium for further 48 h. As shown for a typical experiment, in both MMR^- and MMR^+ HeLa cell lines, MTX caused a decrease in G_2 cells (Fig. 2A, b and d) compared with untreated samples (Fig. 2A, b and c). A fraction of MTX-treated cells

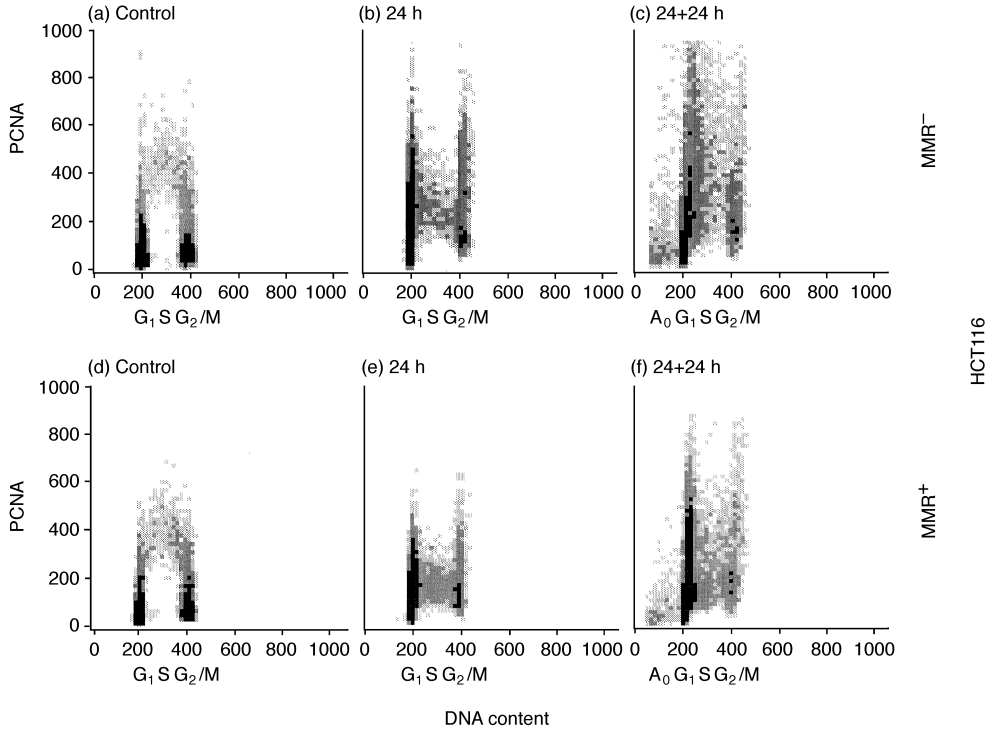

	Control	24 h	24+24 h
G_1	1.0	3.3	6.0
S	6.8	4.0	5.9
G_2/M	1.5	5.4	7.4

MMR^- HCT116

	Control	24 h	24+24 h
G_1	1.0	4.2	5.6
S	6.1	5.2	5.8
G_2/M	1.5	6.3	7.0

MMR^+ HCT116

PCNA Immunofluorescence (a.u.)

Fig. 4. Proliferating Cell Nuclear Antigen (PCNA) immunofluorescence in HCT116 cell lines. (a)–(c): MMR^- parental strain; (d)–(f): MMR^+ strain transfected with chr3. Untreated samples (a) and (d); cells treated with 350 μg/ml MTX for 24 h (b) and (e) or post-incubated for a further 24 h in drug-free medium (c) and (f). Quantitation of PCNA immunofluorescence/cell (arbitrary units, a.u.) is reported.

showed a sub-G_1 DNA content which is typical of apoptotic cells, whose percentage was higher in the MMR^+ cells (approximately 27%) than in the MMR^- cells (approximatley 10%). Cell cycle distribution of MMR^- (HCT116) and MMR^+ (HCT116+chr3) cells showed that both cell lines respond to MTX treatment by an accumulation in S-phase (Fig. 2b, (b) and (d)). However, only MMR-deficient cells showed a decrease in the number of G_2 cells. In MTX-treated cells with restored MMR, we found approximately 9% of cells with a sub-G_1 DNA content. The fraction of apoptotic cells in HCT116 MMR^- cells was significantly lower, reaching approximately 5%.

3.3. MTX stimulates DNA repair synthesis

Fig. 3A shows the biparametric analysis of PCNA immunofluorescence versus DNA content of HeLa cells treated with 250 μg/ml MTX for increasing incubation and/or recovery times. In untreated cells (a), the distribution of detergent-insoluble PCNA is restricted to cells in S phase, where it is involved in replicative DNA synthesis. The quantitation of PCNA immunofluorescence revealed, after a short treatment with MTX (2, 4 and 8 h, corresponding to panels (b)–(d), respectively), an increase in PCNA immunofluorescence in G_1 and in G_2 phases, corresponding to DNA repair synthesis. This phenomenon occurred more markedly after a 24-h treatment with MTX (e), followed by 8 h (f) and 24 h (g) of postincubation in drug-free medium. During the recovery, a fraction of cells showing the sub-G_1 DNA content and basal level of PCNA, representing apoptotic cells, was again found. Biparametric analysis of BrdU immunofluorescence versus DNA content confirmed the PCNA analysis data, showing that untreated cells were actively incorporating

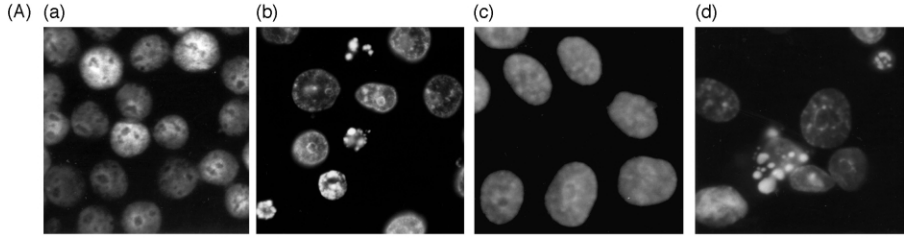

Apoptotic index of MTX-treated cells

Cell line	MMR status	A.I.
HeLa	+	39.87 ± 4.98
	–	14.65 ± 1.32
HCT116	+	12.67 ± 1.70
	–	7.71 ± 0.81

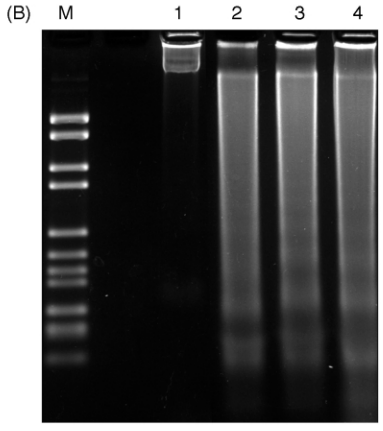

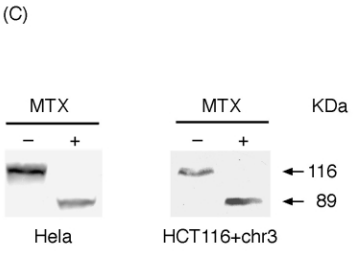

Fig. 5. Apoptotic features of MTX-treated cells. (A) Hoechst 33258 staining of control cells and cells treated for 24 h with 250 (HeLa) or 350 (HCT116) μg/ml MTX and further incubated in fresh medium for 48 h. (a) and (b): HeLa cells; (c) and (d): HCT116+chr3 cells. Apoptotic index (A.I.) is expressed as the mean value of four independent experiments ±standard deviation (S.D.). (B) DNA fragmentation. Genomic DNA was extracted from untreated HeLa cells (lane 1) and from samples harvested after a 24-h treatment with 250 μg/ml MTX followed by a further incubation in drug-free medium for 24 h (lane 2), 48 h (lane 3) or 72 h (lane 4). M: DNA Ladder marker. (C) Western blot analysis of poly (ADP-ribose) polymerase (PARP) proteolysis in MMR^+ HeLa cells incubated for 24 h with 250 μg/ml MTX and recovered in drug-free medium for a further 48 h.

the analogue exclusively during S-phase (Fig. 3B, panel a), while cells treated for 24 h with MTX showed a high BrdU incorporation in G_1 and G_2 phases (Fig. 3B, panel b).

As shown in Fig. 4, in untreated samples from both MMR^- and MMR^+ HCT116 cell lines (a) and (d), PCNA expression was typically confined to S phase. After 24 h of treatment with 350 μg/ml MTX, PCNA was found mainly in the G_1 and G_2 phases (b, MMR^- cells; e, MMR^+ cells). This phenomenon was more evident after a further incubation for 24 h in drug-free medium both in MMR^+ and MMR^- cells ((c) and (f), MMR^- and MMR^+, respectively)).

3.4. Treatment with MTX leads to apoptosis

To verify whether cells with a sub-G_1 DNA content exhibit the classical apoptotic features, we stained MTX-treated MMR^+ cells with Hoechst 33258. Morphological changes typical of apoptosis, such as nuclear shrinkage and chromatin condensation and fragmentation, were visible in both HeLa (Fig. 5A, panel b) and HCT116+chr3 cells (d) after a 24 h-treatment with MTX followed by recovery in fresh medium for 48 h. From the calculation of the apoptotic index (A.I.), it is evident that this parameter was higher for MMR^+ than for MMR^- cells (Fig. 5), as already indicated by the DNA content measurement (Fig. 2).

DNA laddering was investigated by agarose gel electrophoresis of genomic DNA extracted from drug-treated cells. As shown in Fig. 5B for a typical experiment, oligonucleosomal DNA fragments were visible in HeLa cells incubated for 24 h with MTX and further recovered for 24 h (lane 2), 48 h (lane 3) and 72 h (lane 4). Similar results were obtained for HCT116+chr3 cells (data not shown). PARP proteolysis in the treated cells was monitored by western blotting. A typical result is shown in Fig. 5C. The 116 KDa intact protein was present in control cells, while the 89 KDa proteolytic fragment was generated in MTX-treated MMR^+ cells.

In conclusion, we demonstrated that cell death induced by MTX in cells proficient for MMR is associated with typical apoptotic hallmarks, including chromatin condensation, DNA fragmentation and caspase(s) activation. MMR-proficient HeLa and HCT116+chr3 cells activate the apoptotic pathway more efficiently.

4. Discussion

In this study, we investigated cell viability and apoptosis in mismatch repair-proficient and-deficient human cell lines treated with the antifolate drug MTX, which is known to induce base misincorporation [1,2], and hence to trigger DNA repair [11,12]. HeLa cell-clone12 strain, deficient in the MMR protein hPMS2 [18,19], was used in parallel with MMR-competent HeLa cells [16]. Furthermore, we analysed the human colon tumour cell line HCT116 (deficient in the MMR protein hMLH1), and its derivative HCT116+chr3 obtained after the transfer of a normal copy of chromosome 3 to restore MMR activity [17]. All these cell lines were previously characterised with respect to their sensitivity to several DNA damaging agents [17,19,24–27]; however, this is the first attempt to correlate the response to antifolates with the cellular MMR status. In this respect, our results provide the first evidence that the sensitivity of MMR^- cells to antifolate is lower than that of MMR^+ cells. These data are consistent with other reports showing that MMR-deficient cells are resistant to several cytotoxic drugs, including alkylating and methylating agents, platinum compounds and topoisomerase II inhibitors [24–27].

The present finding that in both in MMR^- and MMR^+ cell lines, DNA repair synthesis occurs after MTX treatment, suggests the involvement of repair pathways other than MMR, requiring PCNA. Our results could also be explained by a redundancy among post-replicative DNA mismatch repair pathways, which are independent of a single MMR function [28].

We have found that after MTX treatment, the MMR-proficient cells HCT116+chr3 cells accumulate in S/G_2 phases. Since we observed that MTX-treated HeLa cells are not arrested in S/G_2 phases, it could be possible that, in different cell lines, the MMR system may be connected to different checkpoints. A possible explanation for the different behaviour might take into account the cellular *TP53* status. Indeed, HeLa cells have no functional p53, while HCT116 cells harbour a wild-type(wt)-*TP53* gene. Accordingly, it has been reported that p53 status affects the sensitivity of cells defective for MMR to platinum compounds [29] and alkylating agents [30].

Finally, we observed that, in response to antifolates, apoptosis occurs to a higher extent in MMR^+ cells. Our data are in agreement with the observation that temozolomide-treated MMR^+ cells activate the apoptotic machinery more efficiently than MMR^- cells [31]. The mechanisms by which a functional MMR repair can impair cell survival are still unknown. However, it could be hypothesised that the recognition by MMR proteins of unrepaired or misrepaired lesions can generate a signal capable of activating the apoptotic pathway. It remains to be elucidated how the MMR proteins are involved in DNA damage signalling to the apoptotic machinery.

Acknowledgements

We thank Dr C.R. Boland (University of California, La Jolla, USA) and Dr M. Broggini (Istituto Mario Negri, Milan, Italy) for HCT116 and HCT116+chr3

cell lines. Dr M. Bignami and Dr G. Aquilina (Istituto Superiore di Sanità, Rome, Italy) are kindly acknowledged for the HeLa-clone 12 strain. We are greatly indebted to Dr G. Poirier (Université Laval, Québec, Canada) for the mAb C-2-10 and to Dr A. Lisa (IGBE-CNR, Pavia, Italy) for helpful discussions. I. Frouin is a PhD student (Biologie du Vieillissement, Université Paris VII) supported by the UE contract CHRX CT94 0443. This work was partially supported by Telethon-Italy (Grant no. E.550).

References

1. Huennekens FM. The methotrexate story: a paradigm for development of cancer chemotherapeutic agents. *Adv Enzyme Reg* 1994, **34**, 397–419.
2. Goulian M, Bleile B, Tseng BY. Methotrexate-induced misincorporation of uracil into DNA. *Proc Natl Acad Sci USA* 1980, **77**, 1956–1960.
3. Li JC, Kaminskas E. Accumulation of DNA strand breaks and methotrexate cytotoxicity. *Proc Natl Acad Sci USA* 1984, **81**, 5694–5698.
4. Lorico A, Toffoli G, Boiocchi M, *et al*. Accumulation of DNA strand breaks in cells exposed to methotrexate or N^{10}-propargyl-5,8-dideazafolic acid. *Cancer Res* 1988, **48**, 2036–2041.
5. Frosina G, Fortini P, Rossi O, *et al*. Two pathways for base excision repair in mammalian cells. *J Biol Chem* 1996, **271**, 9573–9578.
6. Lindahl T, Wood RD. Which DNA polymerases are used for DNA-repair in eukaryotes? *Carcinogenesis* 1999, **18**, 605–610.
7. Krokan H, Nilsen H, Skorpen F, Otterlei M, Slupphaug G. Base excision repair of DNA in mammalian cells. *FEBS Lett* 2000, **476**, 73–77.
8. Pascucci B, Stucki M, Jónsson ZO, Dogliotti E, Hübscher U. Long patch base excision repair with purified human proteins. *J Biol Chem* 1999, **274**, 33696–33702.
9. Jónsson ZO, Hübscher U. Proliferating cell nuclear antigen: more than a clamp for DNA polymerases. *BioEssays* 1997, **19**, 967–975.
10. Prosperi E. Multiple roles of the proliferating cell nuclear antigen: DNA replication, repair and cell cycle control. *Prog Cell Cycle Res* 1997, **3**, 193–210.
11. Modrich P, Lahue R. Mismatch repair in replication fidelity, genetic recombination, and cancer biology. *Annu Rev Biochem* 1996, **65**, 101–133.
12. Jiricny J. Replication errors: cha(ll)enging the genome. *EMBO J* 1998, **17**, 6427–6436.
13. Jiricny J, Nystrom-Lahti M. Mismatch repair defects in cancer. *Curr Opin Genetic Dev* 2000, **10**, 157–161.
14. Huschtscha LI, Bartier WA, Andersson Ross CE, Tattersall MHN. Characteristics of cancer cell death after exposure to cytotoxic drugs in vitro. *Br J Cancer* 1996, **73**, 54–60.
15. Tsurusawa M, Saeki K, Fujimoto T. Differential induction of apoptosis on human lymphoblastic leukemia Nalm-6 and Molt-4 cells by various antitumor drugs. *Int J Hematol* 1997, **66**, 79–88.
16. Thomas DC, Roberts JD, Kunkel TA. Heteroduplex repair in extracts of human HeLa cells. *J Biol Chem* 1991, **266**, 3744–3751.
17. Hawn MT, Umar A, Carethers JM, *et al*. Evidence for a connection between the mismatch repair system and the G_2 cell cycle checkpoint. *Cancer Res* 1995, **55**, 3721–3725.
18. Ceccotti S, Aquilina G, Macpherson P, Yamada M, Karran P, Bignami M. Processing of O^6-methylguanine by mismatch correction in human cell extracts. *Current Biol* 1996, **6**, 1528–1531.
19. Ciotta C, Ceccotti S, Aquilina G, *et al*. Increased somatic recombination in methylation tolerant human cells with defective DNA mismatch repair. *J Mol Biol* 1998, **276**, 705–719.
20. Sumner BEH. Trypan blue exclusion test. In *Basic Histochemistry*. Chichester, New York, Brisbane, Toronto, Singapore, John Wiley & Sons, 1988, 24–25.
21. Prosperi E, Stivala LA, Sala E, Scovassi A, Bianchi L. Proliferating cell nuclear antigen complex formation induced by ultraviolet irradiation in human quiescent fibroblasts as detected by immunostaining and flow cytometry. *Exp Cell Res* 1993, **205**, 320–325.
22. Stivala LA, Savio M, Cazzalini O, *et al*. Effect of beta-carotene on cell cycle progression of human fibroblasts. *Carcinogenesis* 1996, **17**, 2395–2401.
23. Donzelli M, Bernardi R, Negri C, *et al*. Apoptosis-prone phenotype of human colon carcinoma cells with a high level amplification of the c-myc gene. *Oncogene* 1999, **18**, 439–448.
24. Carethers JM, Hawn MT, Chauchan DP, *et al*. Competency in mismatch repair prohibits clonal expansion of cancer cells treated with N-methyl-N-nitro-N-nitrosoguanidine. *J Clin Invest* 1996, **98**, 199–206.
25. Davis TW, Wilson-Van Patten C, *et al*. Defective expression of the mismatch repair protein, MLH1, alters G_2-M cell cycle checkpoint arrest following ionizing radiation. *Cancer Res* 1998, **58**, 767–778.
26. Carethers JM, Chauchan DP, Finf D, *et al*. Mismatch repair proficiency and in vitro response to 5-fluorouracil. *Gastroenterology* 1999, **117**, 123–131.
27. Colella G, Marchini S, D'Incalci M, Brown R, Broggini M. Mismatch repair deficiency is associated with resistance to DNA minor groove alkylating agents. *Br J Cancer* 1999, **80**, 338–343.
28. Oda S, Humbert O, Fiumicino S, Bignami M, Karran P. Efficient repair of A/C mismatches in mouse cells deficient in long-patch mismatch repair. *EMBO J* 2000, **19**, 1711–1718.
29. Vikhanskaya F, Colella G, Valenti M, Parodi S, D'Incalci M, Broggini M. Cooperation between p53 and hMLH1 in a human colocarcinoma cell line in response to DNA damage. *Clin Cancer Res* 1999, **5**, 937–941.
30. Aquilina G, Ceccotti S, Martinelli S, *et al*. Mismatch repair and p53 independently affect sensitivity to N-(2-chloroethyl)-N′-cyclohexyl-N-nitrosourea. *Clin Cancer Res* 2000, **6**, 671–680.
31. D'Atri S, Tentori L, Lacal PM, *et al*. Involvement of the mismatch repair system in temozolomide-induced apoptosis. *Mol Pharmacol* 1998, **54**, 334–341.